International Journal of GEOMATE, May, 2018 Vol.14, Issue 45, pp.42-51
Geotec., Const. Mat. & Env., DOI: https://doi.org/10.21660/2018.45.7177
ISSN: 2186-2982 (Print), 2186-2990 (Online), Japan

COMPARISON OF DIFFERENT VEGETATION INDICES FOR ASSESSING MANGROVE DENSITY USING SENTINEL-2 IMAGERY

* Firman Farid Muhsoni[12*], A.B Sambah[34], M. Mahmudi[3], D.G.R Wiadnya[3]

[1]Marine Science Department, University of Trunojoyo Madura, Indonesia

[2]Post-Graduate Program, Faculty of Fisheries and Marine Science, University of Brawijaya Indonesia

[3]Faculty of Fisheries and Marine Science, University of Brawijaya, Indonesia
[4]Marine and Fisheries Resources Exploration & Management Research Group, Brawijaya University, Indonesia

* Corresponding Author: Received: 08 June 2017, Revised: 29 July 2017, Accepted: 25 Aug. 2017

ABSTRACT: Vegetation mapping provides important information for understanding ecological condition through calculation of vegetation density. It based on vegetation indices developed through algorithms of a mathematical model within the visible and near-infrared reflectance bands. The index is an estimate of either leaf density per species or vegetation types, respectively. This study aimed to evaluate those indices and find the best algorithm using Sentinel-2 satellite image. Twenty four algorithms of vegetation indices were analyzed for mangrove density mapping, i.e., BR, GNDVI BR, GR, SAVI, MSAVI, NDRE, NDVI, NDVI2, NDWI, NNIP, PSRI, RR, RVI, VIRE, SVI, VIRRE, MTV1, MTVI2, RDVI, VARI, VI *green*, MSR, and TVI. During pre-processing stage, a digital number of a Sentinel-2 image was converted into radiance and reflectance value. The analysis resulted in three algorithms that provide the highest accuracy, i.e., NDVI (normalized difference vegetation indices) with exponential regression approach, RVI (Ratio Vegetation indices) with the exponential approach and NDVI (normalized difference vegetation indices) with a polynomial approach. The mangrove biomass spatial modeling NDVI with exponential regression approach (RMSE = 89 kg) showed the average of each pixel (10x10m) was 0.97 ton / 100 m2. Total mangrove biomass for above ground and underground vegetation in the study area was 22,365.6 tons. Sentinel-2 satellite image may best use one of those three algorithms, especially applied for mangrove vegetation.

Keywords: Vegetation Indices, Sentinel-2 Imagery, Mangrove Biomass

1. INTRODUCTION

Global warming becomes a global issue. It leads to climate change, due to an increase in atmospheric gas or it was called greenhouse gases. Greenhouse gases occur due to the accumulation of carbon in atmosphere accumulation due to the burning of fossil fuels (the activity of vehicle and industry) [1], [2].

Mangrove has a function as a carbon sink, although the information and data are still relatively minimal [3]. Mangroves are also called mangroves for tree or shrub communities that grow in the coastal area, or they are applied to one type of vegetation species [4]. Mangrove is an intertidal plant found along tropical and non-tropical coastlines [5]. This plant is inundated by tides in the brackish area and has physiological adaptations to salinity [6], [7], [8]. Mangrove ecosystem stored the highest carbon if compared to tropical forests, subtropical forests and boreal forests. Much of the carbon stored in the rich organic underground [7],[9], [10]. Mangrove stores carbon four to five times faster than tropical forests [7];[11]. Climate change is closely related to the existence of forest biomass. Biomass plays a role in the carbon cycle. Forest carbon is stored in forest vegetation. The increase of carbon in the atmosphere caused by the damage or forest fire. More than 50% of the world's mangroves have been destroyed and in the past of two decades, 35% of damage caused by coastal cultivation and development [12]. Mangrove damage has resulted in the contribution of carbon sequestration in the atmosphere [13]. Mangrove area is only 0.7% of the area of tropical forest, but mangrove destruction will supply 10% of CO_2 from the mangrove deforestation [14].

Remote Sensing, flowed by the application of GIS provide quantitative information to investigate the spatial distribution of vegetation, including mangrove forests in the coastal [15]. The application of satellite image analysis has been applied in various ways to illustrate mangrove ecosystems. Some of the published study includes mapping the distribution of mangrove in the coastal, observing mangrove species by ground survey combination, and estimates its structure such as leaf area, canopy height, and biomass [16].

Satellite imagery data is one of the basic information that could describe the location of the deforested area, also healthy vegetation. Satellite remote sensing approach, due to its synoptic, multi-temporal, and multi-spectral ability, can effectively act as one of the methods in providing reliable information on mangrove extent and status of its growth along the coastal areas. The reflectance pattern of the vegetation in red-visible & near infra-red spectral region illustrated the density of all vegetation coverage in the coastal.

Moreover, earth observation satellite like Landsat satellite was commonly applied to define the distribution and density of the mangrove forest [17]. In addition to some satellite applied in vegetation density mapping, Sentinel-2 satellite is a relatively new satellite that is assumed can be used in the mapping of vegetation spatial distribution. Sentinel-2 is a European wide-swath, high-resolution, multi-spectral imaging mission. The full mission specification of the twin satellites flying in the same orbit but phased at 180°, which is designed to give a high revisit frequency of 5 days (temporal resolution) at the Equator [18]. In this study, we analyze Sentinel-2 satellite imagery to investigate and evaluate the density of mangrove forest by calculation of several vegetation indices.

Vegetation mapping provides valuable information for understanding the natural and man-made environment. It is important to obtain vegetation cover in the framework of vegetation protection and restoration programs [19]. Mangrove ecosystems have tremendous relevance to the ecological and economic conditions for conservation and restoration measures. The latest information concerning the extent and condition of mangrove ecosystems is essential for management, policy process, and decision making. It can be solved using remote sensing technology [20]; [21]. The vegetation indices approach in remote sensing is commonly used for vegetation mapping [22]. The vegetation indices have calculated the vegetation density of green leaf and specifically for vegetation species. The purpose of this study is evaluating the different vegetation indices that collected from the Sentinel-2 satellite image analysis.

2. MATERIALS AND METHODS

2.1. Satellite Remote Sensing Data

Sentinel-2 satellite images (Copernicus Sentinel data (2017)) were used in the calculation and mapping of mangrove distribution. The Sentinel-2 satellite has 13 spectral bands from near-infrared to shortwave infrared. Spatial resolution varies from 10m - 60m depending on spectral band [23]. Sentinel 2 image used in this research was December 6, 2016. The bands used in this study were band 2, 3, 4, 5, 6, 8, 8a, with specifications as in Table 1. Moreover, the illustration of Sentinel- 2 spectral bands for 10m and 20m spatial resolution as described in Figure 2 and Figure 3.

Table 1. Sentinel-2 band spesification [4]

No	Band	Wavelength (µm)	Spatial resolution
1	Band 2 – Blue	0.490	10m
2	Band 3 – Green	0.560	10m
3	Band 4 – Red	0.665	10m
4	Band 5 – Vegetation Red Edge	0.704	20m
5	Band 6 – Vegetation Red Edge	0.740	20m
6	Band 8 – NIR	0.835	10m
7	Band 8a – Vegetation Red Edge	0.865	20m

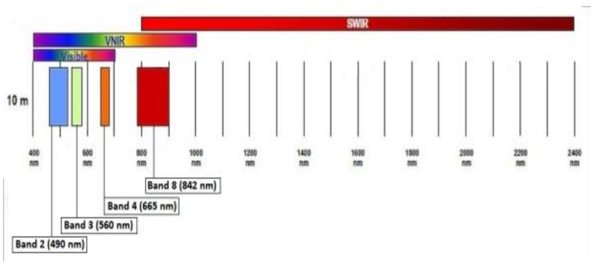

Figure 2. Sentinel-2 10 m spatial resolution bands: B2 (490 nm), B3 (560 nm), B4 (665 nm) and B8 (842 nm) [4]

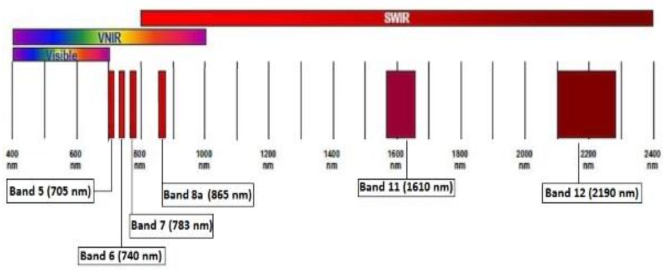

Figure 3. Sentinel-2 20 m spatial resolution bands: B5 (705 nm), B6 (740 nm), B7 (783 nm), B8a (865 nm), B11 (1610 nm) and B12 (2190 nm) [4]

2.2. Radiometry Corrections

The radiometric correction uses the at-sensor reflectance method by changing the pixel value to the radiance-sensor, then converted to at-sensor reflectance, with the following formula [24]:

$$L_x = offset_x + Gain_x \times (BV)_x \quad (1)$$

$$Gain_x = (L_{maks} - L_{min})/BV_{maks} \quad (2)$$

Where, L_χ is the radiance value; BV is Brightness Value; and Offset, Gain from the mathematical calculation of maximum-minimum spectral radiance value in image metadata. The radiance value is changed to the at-sensor reflectance value based on the equation:

$$\rho P = \frac{\pi * L_\chi * d^2}{ESUN_\chi * Cos\theta S} \quad (3)$$

$$d = 1 - 0{,}01674 \cos(0{,}9856(JD - 4)) \quad (4)$$

Where: ρP = the value of at-sensor reflectance; L_χ = radiance value (Wm-2sr-1μm-1); Π = 3,142857142857143; D = distance of earth-sun (astronomical unit); $ESUN_\chi$ = spectral irradiance sun value (Wm-2μm-1); Ɵs = angle sun zenith (degree); JD = Julian Day.

2.3. Transformation of Vegetation Indices

The vegetation indices method that used is structure vegetation indices. The vegetation indices method was also adapted to the images band spectral of Sentinel-2 images. The vegetation indices used in the mapping of mangrove distribution in this study is described in table 2.

Table 2. An appropriate vegetation indices for Sentinel image 2

No	Vegetation Indices
1	BR *(Blue Ratio)*[25],[26] $\left(\frac{\mathbf{R}}{\mathbf{B}}\right) \times \left(\frac{\mathbf{G}}{\mathbf{B}}\right) \times \left(\frac{\mathbf{RE1}}{\mathbf{B}}\right) \times \left(\frac{\mathbf{NIR1}}{\mathbf{B}}\right)$ (5)
2	GNDVI *(Green normalized difference Vegetation indices)* [27] $\frac{\mathbf{NIR1-G}}{\mathbf{NIR1+G}}$ (6)
3	GR *(Green Ratio)* [25] $\frac{\mathbf{G}}{\mathbf{R}}$ (7)
4	SAVI *(Soil-Adjusted Vegetation Indices)* [28], [29], [30] $\frac{\mathbf{(1+0.2)*(NIR1-NIR2)}}{\mathbf{(NIR1+NIR2)+0.2}}$ (8)
5	MSAVI(modified SAVI) [31] $\frac{1}{2}\left[\mathbf{2*NIR1+1}-\sqrt{(\mathbf{2*NIR1+1})^2-\mathbf{8}*(\mathbf{NIR1-R})}\right]$ (9)
6	NDRE *(Normalized difference Red-Edge indices)*[32],[33]. $\frac{\mathbf{NIR1-RE}}{\mathbf{NIR1+RE}}$ (10)
7	NDVI *(normalized difference vegetation indices)*[34],[35],[27] $\frac{\mathbf{NIR1-R}}{\mathbf{NIR1+R}}$ (11)
8	NDVI2 *(normalized difference vegetation indices)* [34] $\frac{\mathbf{NIR2-R}}{\mathbf{NIR2+R}}$ (12)
9	NDWI *(Normalized Difference Water Indices)* [36] $\frac{\mathbf{G-NIR1}}{\mathbf{G+NIR1}}$ (13)
10	NNIP *(Normalized Near Infrared)* [37], [26] $\frac{\mathbf{NIR1}}{\mathbf{(NIR1+R+G)}}$ (14)
11	PSRI *(Plant Senescence Reflectance Indices)*[38] $\frac{\mathbf{R-B}}{\mathbf{RE1}}$ (15)
12	RR (*Red Ratio*) [25] $\left(\frac{\mathbf{NIR1}}{\mathbf{R}}\right) \times \left(\frac{\mathbf{G}}{\mathbf{R}}\right) \times \left(\frac{\mathbf{NIR1}}{\mathbf{REI}}\right)$ (16)
13	RVI *(Ratio Vegetation indices)* [39] $\frac{\mathbf{NIR1}}{\mathbf{R}}$ (17)
14	SVI *(Sentinel Improved Vegetation Indices)* [26] $\frac{\mathbf{NIR2-R}}{\mathbf{NIR2+R}}$ (18)
15	VIRE *(Vegetation Indices based on RedEdge)* [26] $\frac{\mathbf{10.000-NIR1}}{\mathbf{REI^2}}$ (19)
16	VIRRE *(Vegetation Indices Ratio based on RedEdge)* [26] $\frac{\mathbf{NIR1}}{\mathbf{REI}}$ (20)
17	WVVI *(WorldView Improved Vegetative Indices)* [40] $\frac{\mathbf{NIR2-REI}}{\mathbf{NIR2+REI}}$ (21)
18	MTV *(Modified Triangular Vegetation Indices1)* [30] $\mathbf{1,2}*[\mathbf{1,2}*(\mathbf{NIR-G})-\mathbf{2,5}*(\mathbf{R-G})]$ (22)
19	MTV 2 *(Modified Triangular Vegetation Indices2)*[30] $\frac{\mathbf{1.5*(1,2*(NIR-G)-2.5*(R-G))}}{\sqrt{\mathbf{(2*NIR+1)^2-(6*NIR-5*\sqrt{R})}}\mathbf{-0,5}}$ (23)
20	RDVI (*renormalized difference vegetation indices*) [29] $[(\mathbf{NIR-R})/(\mathbf{NIR+R})^2]$ (24)
21	VARI *(vegetation atmospherically resistant indices)*[41] $\frac{\mathbf{(G-R)}}{\mathbf{(G+R-B)}}$ (25)
22	VI *green* [41] $\frac{\mathbf{(G-R)}}{\mathbf{(G+R)}}$ (26)
23	MSR *(Modified Simple Ratio)* [42], [30] $\frac{\left(\left(\frac{\mathbf{NIR}}{\mathbf{R}}\right)\mathbf{-1}\right)}{\left(\left(\frac{\mathbf{NIR}}{\mathbf{R}}\right)\mathbf{+1}\right)^{\mathbf{0.5}}}$ (27)
24	TVI *(triangular vegetation indices)* [39] $\mathbf{0.5}*\left(\mathbf{120}*(\mathbf{NIR-G})\right)-\mathbf{200}*(\mathbf{R-G})$ (28)

Description: Blue (B), Green (G), Red (R), Near-infrared 1 (NIR1), Near-infrared 2 (NIR2), Red Edge 1 (RE1), Red Edge 2 (RE2).

2.4. Estimation of Mangrove Biomass

Estimation of mangrove tree biomass in this study was conducted using allometric equations.

Allometric equations for aboveground biomass [43]; [44] are:

$$W=0.168*\rho*(DBH)^{2.471} \quad (29)$$

Meanwhile, biomass measurements below ground level [7]; [44] are:

$$\boldsymbol{B = 0.199 * \rho^{0.899} * (DBH)^{2.22}} \quad (30)$$

Description:
W = above ground level biomass, B = below ground biomass (kg), ρ = Wood density (g / cm3), DNH = diameter at breast height (cm).

The best vegetation indices search was performed by non-linear regression statistical analysis between biomass and vegetation indices values. Root Mean Square Error (RMSE) is used for determining the best vegetation indices in mangrove biomass estimation. The best regression equation is used to estimate mangrove biomass.

2.5. Study Area

This research was conducted in Majungan Village, Pademawu Sub-district, Pamekasan Regency. This location is located on the Madura Island which is part of East Java Province. The boundary of the study area is in coordinates of $113^0 29'48''$-$113^0 31'24''$ E, $7^0 13'48''$-$7^0 15'12''$ S.

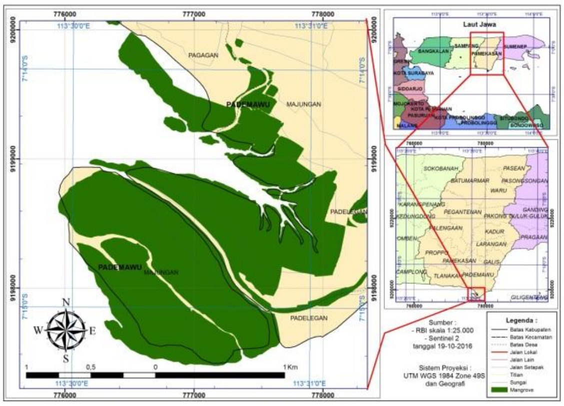

Figure 1. Map of Research Location

3. RESULTS AND DISCUSSION

In this study, the mangrove area was separated by another land cover. The process of mangrove masking was done due to the vegetation indices that was applied to detect canopy density variation, rather than differentiate the type of vegetation. The initial stages of the study began with radiometric correction of sentinel-2 images. The radiometric correction was done by converting radian value to at-sensor reflectance. The corrected image then analyzed the vegetation indices through the calculation of 24 types of vegetation indices (see Table 2). The result of vegetation indices analysis is presented in Table 3.

Table 3. Analysis Results 24 Types of Vegetation Indices.

vegetation indices (Histogram, Min/max/ mean/Stdev)	image of vegetation indices
1.BR 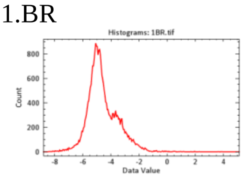 Min =-8.79 , Max = 5.13, Mean =-4.56 ; Stdev = 1.1	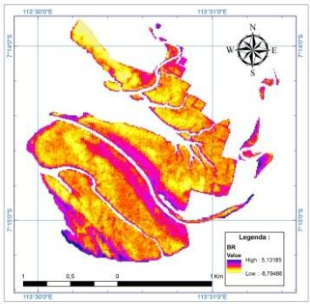
2.GNDVI 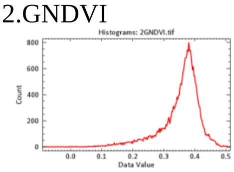 Min = -0.09, Max = 0.52, Mean = 0.35, Stdev = 0.07	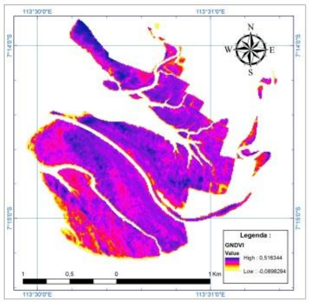
3. GR 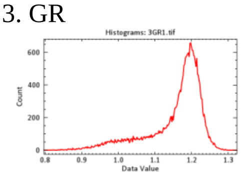 Min = 0.8, Max = 1.32, Mean = 1.16, Stdev = 0.08	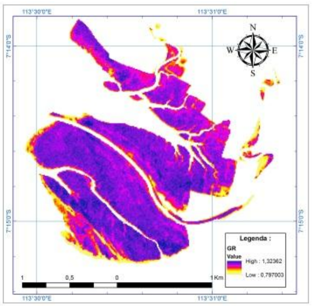
4. SAVI 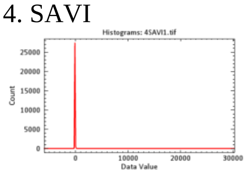 Min = -5943.31, Max = 30299, Mean = -2.02, Stdev = 230.23	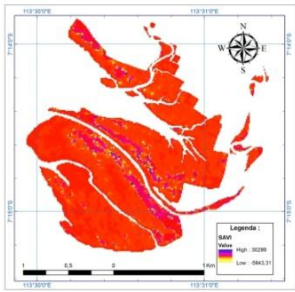

vegetation indices (Histogram, Min/max/ mean/Stdev)	**image of vegetation indices**	**vegetation indices (Histogram, Min/max/ mean/Stdev)**	**image of vegetation indices**
5.MSAVI 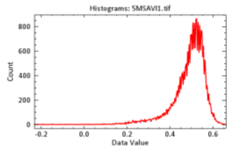 Min = -0.23, Max = 0.66, Mean = 0.49, Stdev = 0.08	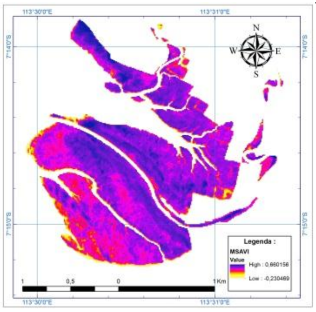	10.NNIP 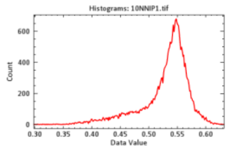 Min = 0.3, Max = 0.63, Mean = 0.53, Stdev = 0.04	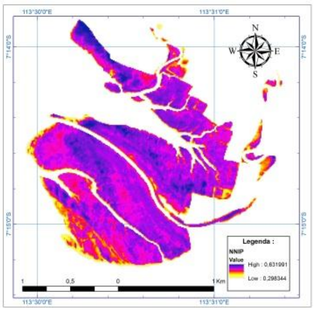
6.NDRE 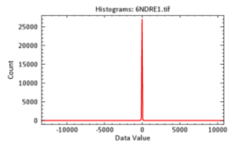 Min = -13367.00, Max = 10940.00, Mean = -4.40, Stdev = 201.74	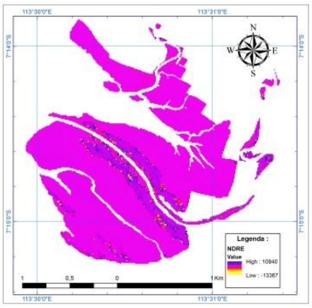	11.PSRI 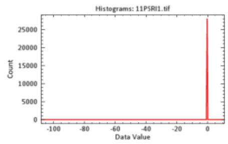 Min = -107.94, Max = 10.88, Mean = 0.05, Stdev = 0.91	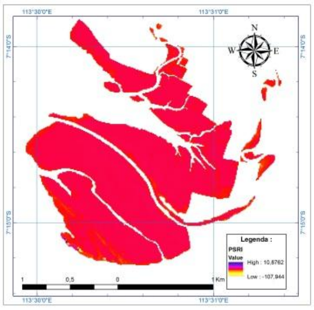
7.NDVI 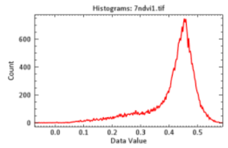 Min = -0.07, Max = 0.59, Mean = 0.41, Stdev = 0.09	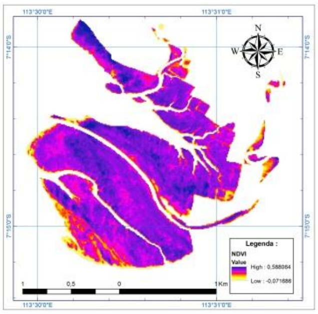	12. RR 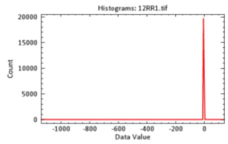 Min = -1138.47, Max = 144.26, Mean = -2.19, Stdev = 12.31	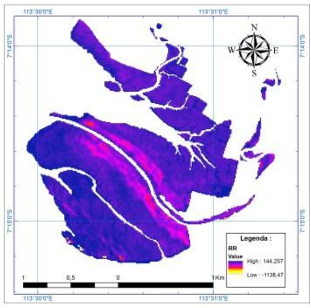
8.NDVI2 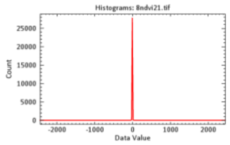 Min = -2442.56, Max = 2449, Mean = 1.56, Stdev = 24.39	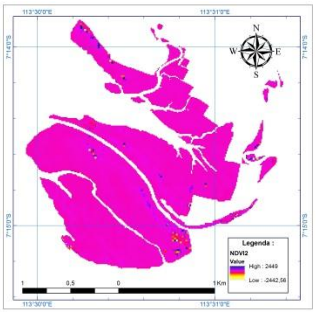	13. RVI 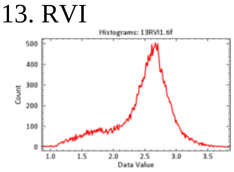 Min = 0.87, Max = 3.86, Mean = 2.48, Stdev = 0.44	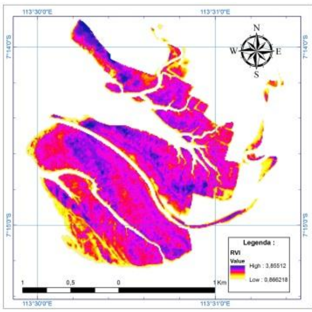
9.NDWI 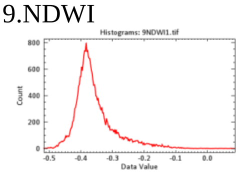 Min = -0.52, Max = 0.09, Mean = -0.35, Stdev = 0.07	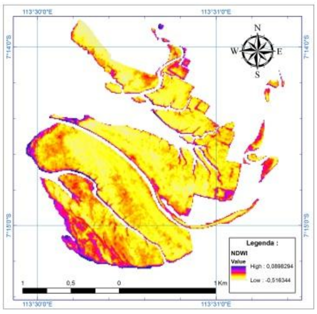	14.SVI 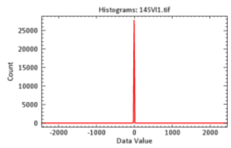 Min = -2442.56, Max = 2449, Mean = 1.56, Stdev = 24.39	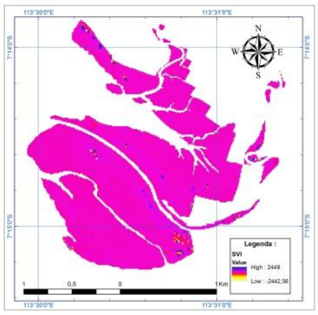

vegetation indices (Histogram, Min/max/ mean/Stdev)	image of vegetation indices	vegetation indices (Histogram, Min/max/ mean/Stdev)	image of vegetation indices
15. VIRE 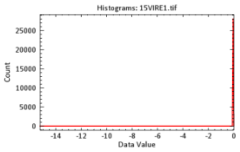 Min = -15.23, Max = 0.0005, Mean = -0.0017, Stdev = 0.14	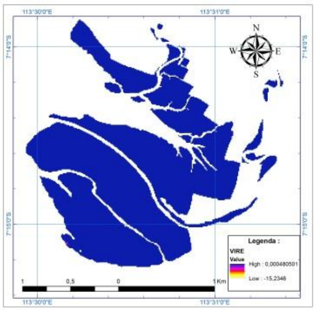	20.RDVI 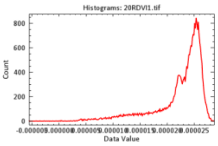 Min = -0.000005, Max = 0.000029, Mean = 0.000022, Stdev = 0.000005	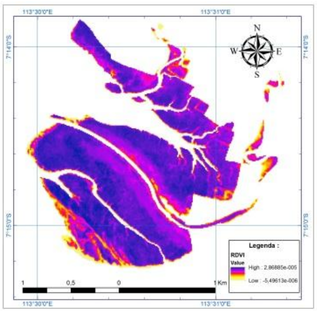
16. VIRRE 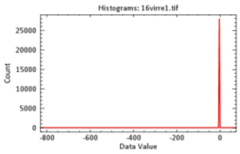 Min = -829.78, Max = 75.02, Mean = -0.82, Stdev = 9.25	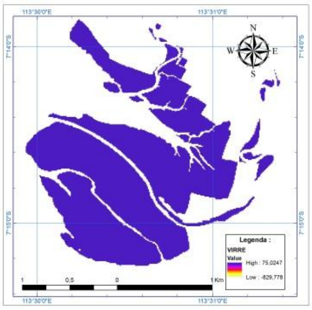	21. VARI 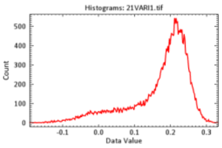 Min = -0.19, Max = 0.33, Mean = 0.17, Stdev = 0.08	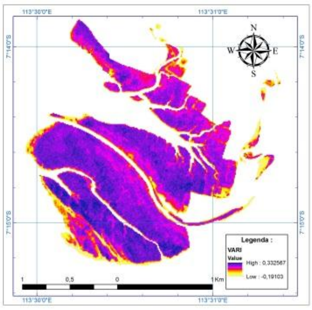
17. WVVI 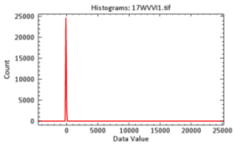 Min = -4546.2, Max = 25214, Mean = 5.21, Stdev = 310.65	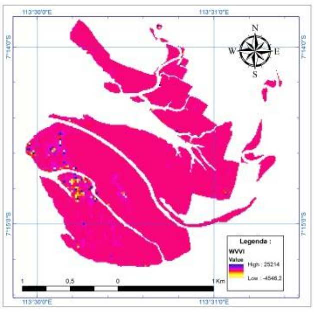	22.VI green 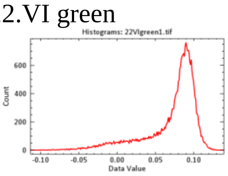 Min = -0.11 , Max = 0.14, Mean = 0.07 , Stdev = 0.03	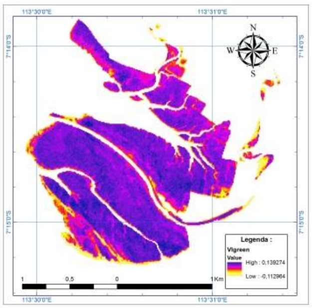
18. MTV 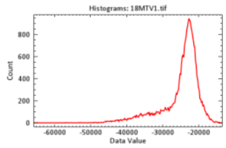 Min = -65734.1, Max = -13520.6, Mean = -24856.8, Stdev = 5439.4	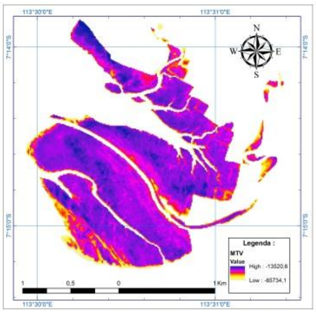	23. MSR 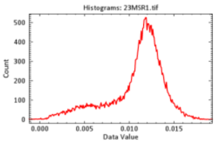 Min = -0.0012, Max = 0.0193, Mean = 0.0109, Stdev = 0.0032	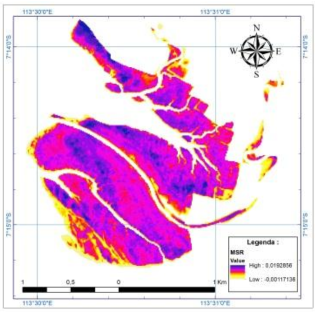
19. MTV2 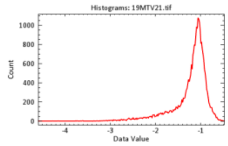 Min = -4.59, Max = -0.48, Mean = -1.22, Stdev = 0.41	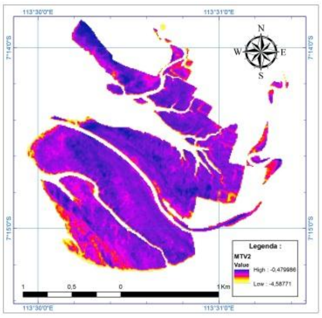	24.TVI 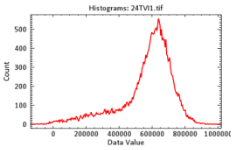 Min = -136940 , Max = 1019240, Mean = 572097.6, Stdev = 160378.9	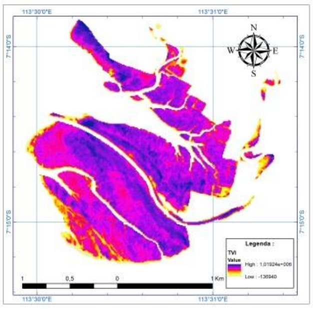

Field measurements were carried out to obtain biomass values of mangrove trees, i.e. above ground biomass values and below ground biomass values. Sampling point field measurement as on the map Figure 4.

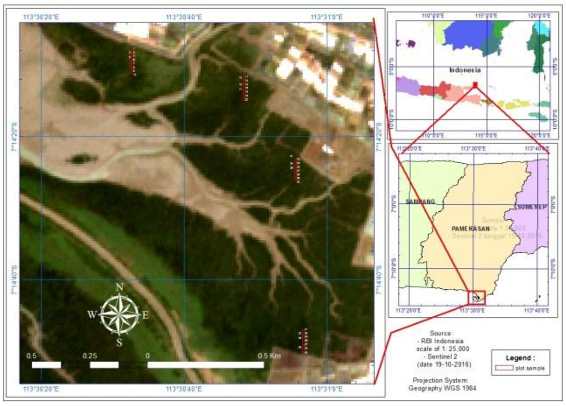

Figure 4. Map of the field measurement sample points

Based on the results of field measurements, biomass mangrove for above ground biomass was 382 kg/100m^2, below ground biomass was 352,7 kg/100m^2 and total biomass was 735 kg/100m^2. In this study, for soil biomass is not taken into account. Table 4 describes the minimum and maximum values of mangrove biomass measured in the field.

Table 4. Mangrove biomass from field data calculation

	Above ground biomass (kg/100m^2)	Below ground biomass (kg/100m^2)	Total biomass (kg/100m^2)
Min	86.9	84.2	171
Max	817.3	754.4	1572
Mean	382.0	352.7	735

The mangrove species found in the sample location plots were *Rhizophora stylosa*, *Rhizophora mucronata*, *Rhizophora apiculata*, *Avicennia marina*, *Aegiceras corniculatum*, *Sonneratia alba*, *Ceriops decandra*, and *Xylocarpus moluccensis*. The composition of dominant mangrove species in the study area was *Aegiceras corniculatum* (32%), *Ceriops decandra* (21.2%), *Rhizophora apiculata* (18.9%), *Sonneratia alba* (12.2%) and *Rhizophora stylosa* (10.7 %).

The next step has analyzed the relationship between image vegetation indices values that have been produced with field measurement data, using logarithmic, quadratic, and exponential regression Field measurement was the measurement of mangrove biomass at the sampling point. The model constructed for biomass estimation was based on the statistical analysis of vegetation indices results of image transformation of Sentinel-2 with the result of biomass calculation value in the field. The regression analysis model used was a non-linear regression. Non-linear regression statistical analysis was based on determination coefficient (R^2). The value of R^2 shows the proportion of the independent variables decrease due to the utilization of the dependent variable information. The range of R^2 is between 0 and 1. It depicting how much dispersion is explained by the prediction. The value of zero means there is no correlation at all, while the value of 1 means the dispersion of the prediction equals the observation. A good R^2 value approaches 1.0 [45]. Root mean square error (RMSE) was used in the best model accuracy test with the lowest error value at the RMSE value [46].

The Kolmogorov-Smirnov normality test was performed before the independent variable used was normally distributed against the dependent variable or not. Normality test results will show normally distributed data when the value of significance on skewness ratio and the kurtosis ratio is in the range -2 to 2. Based on statistical analysis of skewness ratio and the kurtosis ratio value, 24 vegetation indices was spanned between -2 to 2, only 3 Vegetation indices greater than 2, i.e. SAVI, NDVI2, and SVI.

Table 5. Regression results of 24 vegetation indices with R^2 >0.8 value.

Vegetation Indices	Regression Model	Regression Equation	R^2	RMSE (kg)
NDVI	Eksponential	$y = 0.0316e^{22.26x}$	0.859	89
	Polynomial	$y = 86773x^2 - 62664x + 11397$	0.814	353
NNIP	Eksponential	$y = 0.0000001e^{41.24x}$	0.832	459
RVI	Eksponential	$y = 0.09e^{3.40x}$	0.850	352
	Logarithmic	$y = 5534.6\ln(x) - 4538.8$	0.809	510
	Polynomial	$y = 903.25x^2 - 2542.1x + 1215.4$	0.815	397
MTV1	Eksponential	$y = 1485906.17e^{0.00033x}$	0.813	724
MTV2	Eksponential	$y = 180217.44e^{5.32x}$	0.829	452
MSR	Eksponential	$y = 1.7209e^{504.63x}$	0.860	553
	Polynomial	$y = 48,915,274.97x^2 - 812,817.55x + 3,499.67$	0.815	463
TVI	Eksponential	$y = 0.356602e^{0.000012x}$	0.821	2615

The best combination of vegetation indices results can be seen in Table 5. Consistently, the non-linear regression approach through exponential equation shows higher R^2 value than a logarithmic or polynomial equation. The best result of 24 vegetation indices seen from RMSE values was NDVI (normalized difference vegetation indices) with an exponential regression approach (RMSE value = 89 kg). The next decent vegetation indices were RVI (Ratio Vegetation indices) with an exponential approach (RMSE value = 352 kg) and NDVI (normalized difference vegetation indices) with the polynomial (RMSE value = 353 kg), as shown in table 5.

Spatial modeling of mangrove distribution based on vegetation indices was done using NDVI with an exponential regression approach. Mapping of the spatial distribution of mangrove biomass in Pademawu Subdistrict of Pamekasan Regency of East Java Province was based on exponential non-linear regression equation of NDVI vegetation indices. The results of this mapping were illustrated on the map Figure 3.

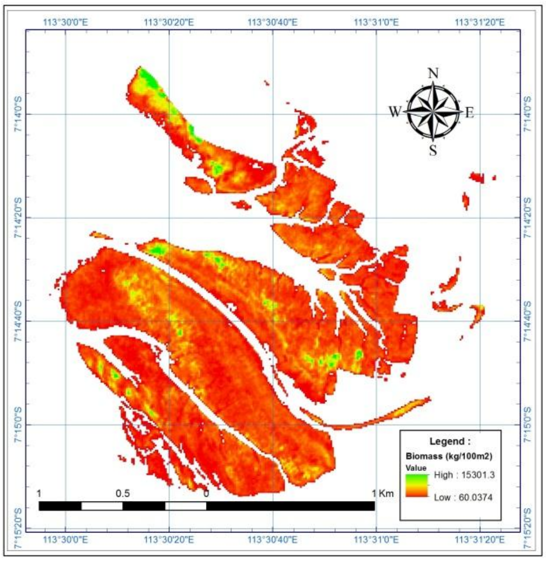

Figure 3. Spatial distribution of biomass in Pademawu Sub-district of Pamekasan Regency of East Java Province based on exponential non-linear regression equation of exponential NDVI vegetation indices.

The result of mangrove biomass spatial modeling showed that the average of mangrove biomass at each pixel (10x10m) was 0.97 ton / 100 m2. Total mangrove biomass for above ground and underground vegetation in the study area was 22,365.6 tons

4. CONCLUSION

The best results of 24 vegetation indices analyzed by exponential regression were NDVI (normalized difference vegetation indices) with exponential regression approach, RVI (Ratio Vegetation indices) with the exponential and NDVI (normalized difference vegetation indices) with the polynomial. The mangrove biomass spatial modeling NDVI with exponential regression approach (RMSE = 89 kg) showed the average of each pixel (10x10m) was 0.97 ton / 100 m2. Total mangrove biomass for above ground and underground vegetation in the study area was 22,365.6 tons.

5. ACKNOWLEDGEMENTS

The author would like to thank the doctoral program of Fishery and Marine Science Faculty of Brawijaya University, Indonesia. The Sentinel-2 image used is a product of Copernicus Sentinel Data, the European Space Agency (ESA).

6. REFERENCES

[1] D. J. Griggs, "Climate change 2001: The scientific basis. The Contribution of Working Group I to the Third Assessment Report of the Intergovernmental Panel on Climate Change," *Weather*, vol. 57, pp. 267–269, 2002.

[2] IPCC, *Climate Change 2001: The Scientific Basis*. The United Kingdom and New York, 2001.

[3] P. G. L. Klinkhamer, "Plant allometry: The scaling of form and process," *Trends Ecol. Evol.*, vol. 10, no. 3, p. 134, 1995.

[4] W. Macnae, "A General Account of the Fauna and Flora of Mangrove Swamps and Forests in the Indo-West-Pacific Region," in *Advances in Marine Biology*, vol. 6, Johannesburg: University of the Witwatersrand, 1969, pp. 73–270.

[5] P. B. Tomlinson, *The Botany of Mangrove*. New York: Cambridge University Press, 1986.

[6] R. R. Lewis, "Ecological engineering for successful management and restoration of mangrove forests," *Ecol. Eng.*, vol. 24, pp. 403–418, 2005.

[7] J. Kauffman and D. Donato, *Protocols for the measurement, monitoring, and reporting of structure, biomass and carbon stocks in mangrove forests*. Bogor, 2012.

[8] T. Dittmar, N. Hertkorn, G. Kattner, and R. J. Lara, "Mangroves, a major source of dissolved organic carbon to the oceans," *Global Biogeochem. Cycles*, vol. 20, no. 1, 2006.

[9] S. E. Page, J. O. Rieley, and C. J. Banks, "Global and regional importance of the tropical peatland carbon pool," *Glob. Chang. Biol.*, vol. 17, no. 2, pp. 798–818, 2011.

[10] A. Hooijer *et al.*, "Current and future CO2 emissions from drained peatlands in Southeast Asia," *Biogeosciences*, vol. 7, no. 5, pp. 1505–1514, 2010.

[11] S. Bouillon, “Carbon cycle: Storage beneath mangroves,” *Nature Geoscience*, vol. 4, no. 5, Nature Publishing Group, pp. 282–283, 2011.
[12] I. C. Feller, C. E. Lovelock, U. Berger, K. L. McKee, S. B. Joye, and M. C. Ball, “Biocomplexity in mangrove ecosystems.,” *Ann. Rev. Mar. Sci.*, vol. 2, pp. 395–417, 2010.
[13] R. S. DeFries, R. a Houghton, M. C. Hansen, C. B. Field, D. Skole, and J. Townshend, “Carbon emissions from tropical deforestation and regrowth based on satellite observations for the 1980s and 1990s.,” *Proceedings of the National Academy of Sciences of the United States of America*, vol. 99, no. 22, pp. 14256–14261, 2002.
[14] D. Alongi and S. Mukhopadhyay, “Contribution of mangroves to coastal carbon cycling in low latitude seas,” *Agric. For. Meteorol.*, vol. 213, pp. 266–272, 2015.
[15] C. Giri and J. Muhlhausen, “Mangrove forest distributions and dynamics in Madagascar (1975-2005),” *Sensors*, vol. 8, no. 4, pp. 2104–2117, 2008.
[16] B. W. Heumann, “An object-based classification of mangroves using a hybrid decision tree-support vector machine approach,” *Remote Sens.*, vol. 3, no. 11, pp. 2440–2460, 2011.
[17] S. Sremongkontip, Y. Hussin, and L. Groenindijk, “Detecting changes in the mangrove forests of southern Thailand using remotely sensed data and GIS,” *Int. Arch. Photogramm. Remote Sens.*, vol. 33, no. Part B7, pp. 567–574, 2000.
[18] SUHET, *SENTINEL-2 User Handbook*, no. 1. https://earth.esa.int/web/sentinel/user-guides/sentinel-2-msi/resolutions/spatial, 2015.
[19] Y. Xie, Z. Sha, and M. Yu, “Remote sensing imagery in vegetation mapping: a review,” *J. Plant Ecol.*, vol. 1, no. 1, pp. 9–23, 2008.
[20] L. Wang and W. P. Sousa, “Distinguishing mangrove species with laboratory measurements of hyperspectral leaf reflectance,” *Int. J. Remote Sens.*, vol. 30, no. 5, pp. 1267–1281, 2009.
[21] C. Kuenzer, A. Bluemel, S. Gebhardt, T. V. Quoc, and S. Dech, “Remote sensing of mangrove ecosystems: A review,” *Remote Sens.*, vol. 3, no. 5, pp. 878–928, 2011.
[22] M. A. El-Shirbeny, B. Abdellatif, A.-E. M. Ali, and N. H. Saleh, “Evaluation of Hargreaves based on remote sensing method to estimate potential crop evapotranspiration,” *Int. J. GEOMATE*, vol. 11, no. 23, pp. 2143–2149, 2016.
[23] M. Drusch *et al.*, “Sentinel-2: ESA’s Optical High-Resolution Mission for GMES Operational Services,” *Remote Sens. Environ.*, vol. 120, pp. 25–36, 2012.
[24] T. M. Lillesand, R. W. Kiefer, and J. W. Chipman, *Remote Sensing and Image Interpretation*. Wiley, 2004.
[25] L. T. Waser, M. Küchler, K. Jütte, and T. Stampfer, “Evaluating the potential of worldview-2 data to classify tree species and different levels of ash mortality,” *Remote Sens.*, vol. 6, no. 5, pp. 4515–4545, 2014.
[26] W.-T. Ng, P. Rima, K. Einzmann, M. Immitzer, C. Atzberger, and S. Eckert, “Assessing the Potential of Sentinel-2 and Pléiades Data for the Detection of Prosopis and Vachellia spp. in Kenya,” *Remote Sens.*, vol. 9, no. 1, p. 74, 2017.
[27] a. a. Gitelson and M. N. Merzlyak, “Remote estimation of chlorophyll content in higher plant leaves,” *Int. J. Remote Sens.*, vol. 18, no. 12, pp. 2691–2697, 1997.
[28] A. R. Huete, “A soil-adjusted vegetation index (SAVI),” *Remote Sens. Environ.*, vol. 25, no. 3, pp. 295–309, 1988.
[29] J. L. Roujean and F. M. Breon, “Estimating PAR absorbed by vegetation from bidirectional reflectance measurements,” *Remote Sens. Environ.*, vol. 51, no. 3, pp. 375–384, 1995.
[30] D. Haboudane, J. R. Miller, E. Pattey, P. J. Zarco-Tejada, and I. B. Strachan, “Hyperspectral vegetation indices and novel algorithms for predicting green LAI of crop canopies: Modeling and validation in the context of precision agriculture,” *Remote Sens. Environ.*, vol. 90, no. 3, pp. 337–352, 2004.
[31] J. Qi, A. Chehbouni, A. R. Huete, Y. H. Kerr, and S. Sorooshian, “A modified soil adjusted vegetation index,” *Remote Sens. Environ.*, vol. 48, no. 2, pp. 119–126, 1994.
[32] J. U. H. Eitel *et al.*, “Broadband, red-edge information from satellites improves early stress detection in a New Mexico conifer woodland,” *Remote Sens. Environ.*, vol. 115, no. 12, pp. 3640–3646, 2011.
[33] A. Ramoelo, S. Dzikiti, H. Van Deventer, A. Maherry, M. A. Cho, and M. Gush, “Potential to monitor plant stress using remote sensing tools,” *J. Arid Environ.*, vol. 113, pp. 134–144, 2015.
[34] J. W. Rouse, R. H. Haas, J. A. Schell, and D. W. Deering, “Monitoring the vernal advancement and retrogradation (green wave effect) of natural vegetation,” *Prog. Rep. RSC 1978-1*, p. 112, 1973.
[35] N. Pettorelli *et al.*, “The Normalized Difference Vegetation Index (NDVI): Unforeseen successes in animal ecology,” *Clim. Res.*, vol. 46, no. 1, pp. 15–27, 2011.
[36] B. C. Gao, “NDWI - A normalized difference

water index for remote sensing of vegetation liquid water from space," *Remote Sens. Environ.*, vol. 58, no. 3, pp. 257–266, 1996.

[37] R. P. Sripada, R. W. Heiniger, J. G. White, and R. Weisz, "Aerial Color Infrared Photography for Determining Late-Season Nitrogen Requirements in Corn," *Agron. J.*, vol. 97, pp. 1443–1451, 2005.

[38] M. N. Merzlyak, A. a Gitelson, O. B. Chivkunova, and V. Y. U. Rakitin, "Non-destructive optical detection of pigment changes during leaf senescence and fruit ripening," *Physiol. Plant.*, vol. 106, no. 1, pp. 135–141, 1999.

[39] N. H. Broge and E. Leblanc, "Comparing prediction power and stability of broadband and hyperspectral vegetation indices for estimation of green leaf area index and canopy chlorophyll density," *Remote Sens. Environ.*, vol. 76, no. 2, pp. 156–172, 2001.

[40] A. F. Wolf, "Using WorldView-2 Vis-NIR multispectral imagery to support land mapping and feature extraction using normalized difference index ratios," in *Algorithms and Technologies for Multispectral, Hyperspectral, and Ultraspectral Imagery XVIII*, 2012, vol. 8390, p. 83900N–83900N–8.

[41] A. a Gitelson, Y. Zur, O. B. Chivkunova, and M. N. Merzlyak, "Assessing carotenoid content in plant leaves with reflectance spectroscopy.," *Photochem. Photobiol.*, vol. 75, no. 3, pp. 272–281, 2002.

[42] J. M. Chen, "Evaluation of vegetation indices and a modified simple ratio for boreal applications," *Can. J. Remote Sens.*, vol. 22, no. 3, pp. 229–242, 1996.

[43] J. Chave *et al.*, "Tree allometry and improved estimation of carbon stocks and balance in tropical forests," *Oecologia*, vol. 145, no. 1, pp. 87–99, 2005.

[44] A. Komiyama, J. E. Ong, and S. Poungparn, "Allometry, biomass, and productivity of mangrove forests: A review," *Aquat. Bot.*, vol. 89, no. 2, pp. 128–137, 2008.

[45] P. Krause and D. P. Boyle, "Advances in Geosciences Comparison of different efficiency criteria for hydrological model assessment," *Adv. Geosci.*, vol. 5, no. 89, pp. 89–97, 2005.

[46] M. Yan *et al.*, "Simulation of Forest Carbon Fluxes Using Model Incorporation and Data Assimilation," *Remote Sens.*, vol. 8, no. 7, p. 567, 2016.